

LAI retrieval from SPOT Vegetation in Mediterranean basins

Benedetto Figorito, Eufemia Tarantino, Gabriella Balacco, Andrea Gioia, Vito Iacobellis

Politecnico di Bari, via Orabona 4, Bari, 70125, Italy, e-mail: e.tarantino@poliba.it

Abstract. Distributed hydrological models exploit several variables and parameters, that are subject to complex space-time patterns. An important role is played by the representation of vegetation dynamics and, in many conceptual watershed models, vegetation indices (VI) are used, in order to provide a quantitative measure of vegetation conditions, that are often obtained through the combination of different spectral channels of remote sensing data. Usually, the simple structure of VIs enables their retrieval from different sensor systems, which on one hand allow for the comparison of different products, on the other hand ensure the length and continuity of critical datasets for continuous simulation of land surface processes and climate change studies. In this work the vegetation dynamic trends during 1999-2010 in the North of the Apulia region (Southern Italy) were analyzed using SPOT VGT sensor data. Three bands of VEGETATION (red, NIR, and SWIR) were used to implement the vegetation index named Reduced Simple Ratio (RSR) to derive leaf area index (LAI). The average LAI is an indicator of biomass and canopy cover, while the difference between the annual maximum and minimum LAI is an indicator of annual leaf turnover. Linear regression analysis of the space-time distribution of LAI at the catchment scale was performed over the examined period to detect the consistency of vegetation dynamics in the study area.

Keywords. Leaf area index, SPOT VGT, time series analysis

1. Introduction

The importance of mapping, quantifying and monitoring changes in the physical characteristics of vegetation cover have become essential to understanding dynamics of state variables for hydrologic, agricultural and ecologic systems from regional to global scales [17; 18; 28].

The long-term operational satellite missions, based on both active and passive sensors, have provided an increasing amount of information, which requires advanced and effective methodological approaches to combine digital image-processing techniques with observational time series analysis [26] in order to obtain information on features and causes of variations at different time scales [24; 8].

Even if multitemporal coarse resolution satellite images clearly restricts the range of spatial details that can be detected, they have proved to be suitable for identifying locations of rapid change for further analysis with higher resolution data [10]. However, extracting trends from time series can be challenging due to short-term (e.g., phenological) variations in the data or overall low signal-to-noise-ratios [27]. It is hence necessary to establish long enough time series for a reliable critical historical perspective on vegetation activities [4; 21] to determine indicators of the degree of stress as consequence of natural hazards and/or anthropogenic activities [25].

On the other hand, the detail and frequency of acquisition of multitemporal coarse resolution satellite images appear suitable for their exploitation within hydrological models applied at the basin scale. In a semi-arid Mediterranean environment, the hydrological water balance is highly conditioned by land cover and vegetation dynamics. For example, evapotranspiration, which is recognized as the main hydrologic loss (50÷60% of mean annual rainfall), can be evaluated as the sum of two distinct processes: evaporation from bare soil and transpiration from vegetative soil. In drought

conditions, the evaporation from bare soil increases, while canopy transpiration generally decreases. Therefore, space-time distribution of vegetation is a key factor for a correct evaluation of evapotranspiration [9] and also for understanding climate-soil-vegetation interactions [19].

The total leaf area quantity per unit area, namely the leaf area index (LAI), responds rapidly to different stress factors and changes in climatic conditions, proving very useful as consistent indicator to characterize the vegetation condition [7; 23; 12; 29] commonly used in hydrologic and climate models.

In this paper, time series SPOT VGT satellite archives were used for retrieving Leaf Area Index (LAI) on a study area located in the North of the Apulia region (Italy). The variability in space and time of the leaf area index (LAI) at the catchment scale over the period 1999-2010 was analyzed, to detect the consistency of vegetation dynamics and to characterize the vegetation condition to be used in hydrologic and climate models.

2. LAI estimates from coarse resolution sensor data

Data on estimates of LAI worldwide are needed by the scientific community investigating global scale fluxes and energy balance of the land surface. In fact, LAI provides an indicator of vegetation growth cycle and, as such, of the plant activity in terms of water transpiration [9].

Measuring LAI is not a straightforward task, especially over a heterogeneous landscape [16]. LAI assumes different values according to belonging species and for the same species it varies with the stage of development and the crop technique.

A number of global LAI products are being routinely estimated using data of spatial moderate and coarse-resolution from various satellite sensors such as Moderate Resolution Imaging Spectroradiometer (MODIS), Système Probatoire d'Observation de la Terre VEGETATION (SPOT VGT), National Oceanic and Atmospheric Administration (NOAA) Advanced Very High Resolution Radiometer (AVHRR) and Medium Resolution Imaging Spectrometer (MERIS). The global LAI products produced from MODIS, SPOT and MERIS data have a frequency of 1–2 weeks and cover timely a period of somewhat more than one decade [20]. Validation of these products is a difficult task because ground-based plot measurements are always limited and cannot be compared with these image data directly without considering the surface heterogeneity. Major issues facing LAI product validation may include: (1) consistency in ground-based LAI measurement methods and protocols since there have been different definitions of LAI and diverse methods of LAI estimation; (2) methods for spatial scaling from ground plot to pixel; (3) accuracy assessment for coarse-resolution LAI images [6].

For LAI estimation some spectral vegetation indexes using the ratio of some combination of red and near-infrared (NIR) reflectance, such as the normalised difference vegetation index (NDVI) or the simple ratio (SR), are commonly used [23], even if some studies suggested that NDVI and LAI are strongly correlated [1].

Chen *et al.* [6] made use of the RSR based on a previous study documenting its ability to deal with heterogeneous land covers. Three bands of SPOT-VEGETATION (red, NIR, and SWIR) were used to form a vegetation index named reduced simple ratio (RSR). It is defined as follows [3]:

$$RSR = \frac{\rho_{NIR}}{\rho_{RED}} \left(1 - \frac{\rho_{SWIR} - \rho_{SWIRmin}}{\rho_{SWIRmax} - \rho_{SWIRmin}} \right) \quad (1)$$

where:

- ρ_{NIR} , ρ_{RED} , and ρ_{SWIR} are the reflectance in NIR, RED, and SWIR band, respectively.

- ρ_{SWIRmin} and ρ_{SWIRmax} are the minimum and maximum SWIR reflectance found in each image and defined as the 1% minimum and maximum cutoff points in the histograms of SWIR reflectance in a wide scene.

The major advantages of RSR can be summarized as follows:

- the difference between cover types is very much reduced so that the accuracy for LAI retrieval for mixed cover types can be improved or a single LAI algorithm can be developed without resorting to a coregistered land cover map as the first approximation.
- the background (understory, moss cover, litter, and soil) influence is suppressed using RSR because the SWIR band is most sensitive to the amount of vegetation containing liquid water in the background [3].

For LAI calculations of cropland, grassland, tundra, barren, urban, the algorithm was based on RSR:

$$\text{LAI} = \text{RSR}/1.3 \quad (2)$$

By using RSR, the background value is no longer needed. However, this does not mean that the background effect is completely removed. The extent to which the background effect is suppressed depends on how well the minimum SWIR represents reflectance for the whole scene.

3. Methods

3.1. Study area

The study area is in Puglia, the most Eastern region of Italy overlooking the Adriatic and Ionian seas. More precisely, it includes the Gargano area, the river basins Candelaro, Cervaro, Carapelle, Ofanto and the reclamation ground of Margherita di Savoia surrounded by the coast line and the watersheds of Ofanto and Carapelle .

The study area, in the North of the region, is characterized by heterogeneous climate that range from semi-arid to humid, the low plain is called “Tavoliere delle Puglie” which the second Italian plain in size and has agriculture as the first productive activity. It includes arable lands producing cereals and vegetables, century-old olive groves, fruit orchards and vineyards, together with spontaneous vegetation typical of Mediterranean Macchia.

The climate is typically Mediterranean, with a strong interannual variability and a marked annual seasonality. The average rainfall minimum value is about 600 mm per year; rainfall is distributed quite irregularly over the year, with average peaks in the October-March semester.

A marked differentiation exists between seasonal and permanent native vegetation (for instance between winter wheat and olives). Seasonal wheat crops are usually characterized by an almost complete vegetation ground cover with a high root density and shallow root depth.

Instead, permanent tree crops, mainly olives, grapes, and citrus, have lower percentages of vegetation ground cover, deeper roots and lower root density.

The spacing of trees is affected by local agricultural practices aimed at maximizing productivity and reducing disease exposure.



Figure 1. Location of the study area in the North of the Puglia region (Italy) including the basins of rivers Candelaro, Cervaro, Carapelle and Ofanto.

3.2. Pre-processing of SPOT- VGT data

The freely available SPOT VGT-S RADIOMETRY product covering Europe (25_N-75_N, -11_E-62_E) was acquired for the investigated period (144 scenes totally).

The VEGETATION (VGT) instrument encompasses 4 spectral bands in the blue, red, near infrared and shortwave infrared spectral wavelengths. The orbit of the VGT sensor ensures daily global coverage of the Earth's surface with a 1km footprint. The Vlaamse Instelling voor Technologisch Onderzoek (VITO) (www.vgt.vito.be) routinely operates atmospheric and angular corrections of reflectance data from SPOT-4/VGT-I and SPOT-5/VGTII, which results in two 10-day composite products (S10 and D10 data) delivered in a Plate-Carrée projection (WGS84 ellipsoid), at a spatial resolution of $1/112^\circ$ [15].

To facilitate the comparison of multi-date imagery it was necessary to register both data sets in a single map coordinate system, in this case Universal Transverse Mercator projection (zone 33) and datum WGS84.

Each composite product consists of two 8-bit data files: a digital number (DN) file to be converted into NDVI and a status map (SM) file describing some potential problems observed for the reflectance of each band during the period of compositing [11]. Using 12 years (from January 1, 1999 to December 31, 2010) of VGT data, we preferentially used S10 data. VGT-S10 products (ten day synthesis) are compiled by merging segments (data strips) acquired in a ten days. All the segments of this period are compared again pixel by pixel to pick out the 'best' ground reflectance values. These products provide data from all spectral bands, the NDVI and auxiliary data on image acquisition parameters [14].

There are nearly always disturbances in VGT time series data, caused by cloud contamination, atmospheric variability, and bi-directional effects. These disturbances greatly affect the monitoring

of land cover and terrestrial ecosystems and show up as undesirable noise. In this work, Savitzky–Golay filter was used to reduce cloud contamination and atmospheric variability [5].

3.3. Linear regression analysis for detection of space-time patterns

The method of linear regression analysis is widely used in vegetation dynamics detection with time series data. In the method, time t was set as the independent variable with VI value of each pixel for dependent variable, and the slope of linear regression was an efficacious index quantifying the trend of vegetation dynamics in the study period. In details, plus value of the slope refers to positive trend of vegetation dynamics, which means increasing of vegetation coverage or enhancing of vegetation activity; and minus value of the slope refers to negative trend of vegetation dynamics, which means decreasing of vegetation coverage or weakening of vegetation activity.

The calculation of the slope was as follows:

$$\text{Slope} = \frac{n \sum_{i=1}^n i * LAI_i - (\sum_{i=1}^n i) (\sum_{i=1}^n LAI_i)}{n \sum_{i=1}^n i^2 - (\sum_{i=1}^n i)^2} \quad (3)$$

where

- n is the number of years in the study period,
- i is the serial number of the year
- LAI_i is LAI value in the year i .

The goodness of fit of the linear regression was provided by the coefficient of determination R^2 which is in this case equal to the square correlation coefficient (r).evaluated as:

$$r = \frac{\text{cov}(i, LAI_i)}{\sqrt{\text{Var}(i) \text{Var}(LAI_i)}} \quad (4)$$

where i is the serial number of the year in the study period, LAI_i is LAI value in the year i , cov indicates the covariance, and Var is the variance.

Moreover, a significance test of vegetation dynamic trend was conducted using the p-value statistic with a significance level of 0.05.

4. Results and discussion

The linear regression analysis was performed considering the time series of annual LAI values for any pixel (1 km^2) included in the study area. Figure 2 represents the linear trends observed over the 12-years row studied, obtained for each pixel in terms of LAI annual average, standard deviation and coefficient of variation. Both the average and the standard deviation show a significant positive trend in large areas, as confirmed by the maps of p-value and R^2 , especially in the valleys of the river basins studied and in the Tavoliere plain. A significant increase of the coefficient of variation was also observed but only in a reduced number of pixels. This means that a good number of pixels observe the increase of both mean and standard deviation values of the annual distribution of LAI. The subplots in Figure 2 also show, in terms of R^2 and p-value, that a remarkable increase of the annual mean LAI value is widely and almost homogeneously observed in the Tavoliere plain.

The whole study area, indeed, shows a remarkable percentage of area with positive trend (about 54 %), with maximum values of 75 % in the Margherita di S. reclamation ground, followed by the Gargano and Candelaro areas with 66 % (see Table 1).

In order to analyze the effect of land-use on the increase of LAI the map resolution was uniformly downscaled to cells of 90 m x 90 m. The land-use maps of S.I.G.R.I.A. [13] was used for this purpose.

Table 1 also shows the areal land-use distribution for the six areas shown in Figure 1 and the percentage of the same land-uses within the area (A+) with positive trend of the annual mean LAI. The percentages of land-use in the areas with positive trends shown in Table 1 at a first glance seem to reflect the dominant distribution of land-use observed in the different areas, nevertheless, some differences between the percentage of land-use in the whole basin and the percentage of land-use in the area with positive trend suggest that different behaviors occur ranging from the Northern areas towards the Southern part of the study area.

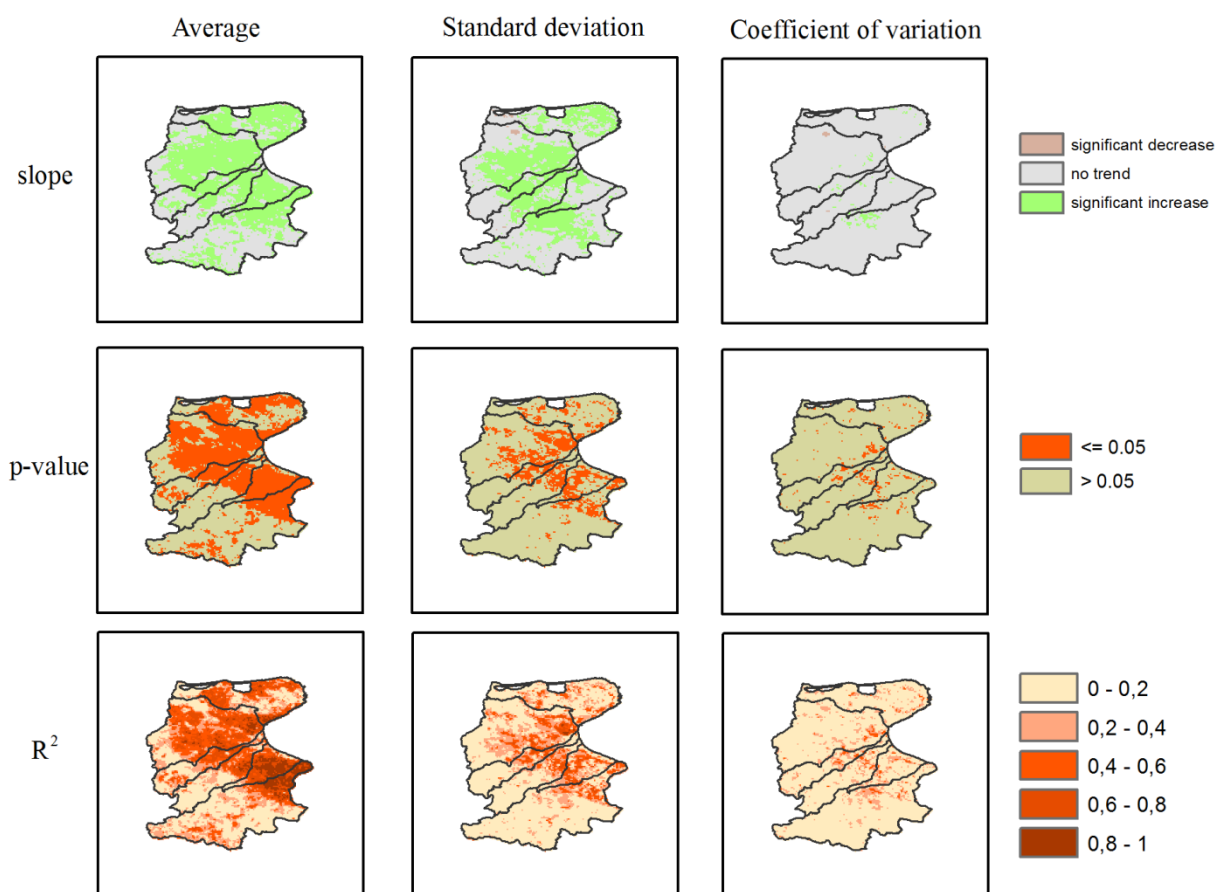


Figure 2. LAI linear trends observed over the 12 years studied, obtained for each pixel annually.

The Gargano area, in fact, is the only one where natural vegetation (mainly woods) dominates the area with positive trend with respect to other land covers. It is, instead, the agricultural vegetation to mainly explain the increase of LAI in all remaining basins. In particular a significant increase of the mean LAI characterizes the wheat areas of the Candelaro and Cervaro basin. A significant increase of the mean LAI is observed in vegetables of Cervaro and Carapelle basins while an increase of LAI in fruit trees is observed in all the basins and particularly the areas of Margherita di S. and of the Ofanto river.

This general behavior can be explained by considering that the last few years of this 12-years row (1999-2010) were characterized by increased annual amounts and variability of rainfall. This climatic forcing is then reflected by both the natural systems and the human action in terms of agricultural practice and management.

Nevertheless more investigation is needed in order to quantitatively correlate the LAI behavior with the rainfall variability and also to further explain the geomorphological effects in the positive trend of LAI.

Table 1. Land-use distribution in study area and in areas (A+) with positive trend of annual average LAI.

Study area		Gargano		Candelaro		Cervaro		Carapelle		Margherita di S.		Ofanto	
A [km ²]	A+ [%]	A [km ²]	A+ [%]	A [km ²]	A+ [%]	A [km ²]	A+ [%]	A [km ²]	A+ [%]	A [km ²]	A+ [%]	A [km ²]	A+ [%]
8951	54.2	1427	65.9	2331	65.5	787	46.4	987	45.2	616	74.9	2803	39.6
Land Use		% of A	% of A+										
Natural vegetation (woods)		63.5	72.3	10.6	8.2	18.0	12.9	9.4	3.4	0.5	0.2	20.8	18.9
Wheat and other cereals		10.4	7.3	61.1	65.1	63.8	67.5	73.4	73.5	33.4	34.0	51.8	43.2
Fruit trees (olive, grape, citrus, etc)		11.6	14.3	12.4	12.6	5.3	7.7	6.6	9.3	40.0	48.2	13.2	24.8
Vegetables		7.2	0.8	9.4	9.4	7.6	8.4	7.7	11.7	14.2	14.7	8.5	8.0
Other vegetated areas		5.7	4.7	4.5	3.3	2.8	2.2	1.9	1.6	9.6	1.7	4.0	4.0
Urban areas		1.6	0.5	2.1	1.5	2.4	1.4	1.1	0.6	2.3	1.1	1.7	1.2

References

- [1] Andersen, J., Dybkjaer, G., Jensen, K.H., Refsgaard, J. & Rasmussen, K., 2002. *Use of remotely sensed precipitation and leaf area index in a distributed hydrological model*. Journal of Hydrology, 264 (1), 34-50.
- [2] Asrar, G., Fuchs, M., Kanemasu, E. & Hatfield, J., 1984. *Estimating absorbed photosynthetic radiation and leaf area index from spectral reflectance in wheat*. Agronomy Journal, 76 (2), 300-306.
- [3] Brown, L., Chen, J.M., Leblanc, S.G. & Cihlar, J., 2000. *A shortwave infrared modification to the simple ratio for lai retrieval in boreal forests: An image and model analysis*. Remote Sensing of Environment, 71 (1), 16-25.
- [4] Brown, M.E., Pinzón, J.E., Didan, K., Morisette, J.T. & Tucker, C.J., 2006. *Evaluation of the consistency of long-term ndvi time series derived from AVHRR, SPOT-VEGETATION, SEAWIFS, MODIS, AND LANDSAT ETM+ sensors*. Geoscience and Remote Sensing, IEEE Transactions on, 44 (7), 1787-1793.
- [5] Chen, J., Jönsson, P., Tamura, M., Gu, Z., Matsushita, B. & Eklundh, L., 2004. *A simple method for reconstructing a high-quality ndvi time-series data set based on the Savitzky–Golay filter*. Remote Sensing of Environment, 91 (3), 332-344.
- [6] Chen, J.M., Pavlic, G., Brown, L., Cihlar, J., Leblanc, S., White, H., Hall, R., Peddle, D., King, D. & Trofymow, J., 2002. *Derivation and validation of canada-wide coarse-resolution leaf area index maps using high-resolution satellite imagery and ground measurements*. Remote Sensing of Environment, 80 (1), 165-184.
- [7] Fassnacht, K.S., Gower, S.T., Mackenzie, M.D., Nordheim, E.V. & Lillesand, T.M., 1997. *Estimating the leaf area index of north central wisconsin forests using the LANDSAT thematic mapper*. Remote Sensing of Environment, 61 (2), 229-245.
- [8] Gessner, U., Niklaus, M., Kuenzer, C. & Dech, S., 2013. *Intercomparison of leaf area index products for a gradient of sub-humid to arid environments in west africa*. Remote Sensing, 5 (3), 1235-1257.
- [9] Gigante, V., Iacobellis, V., Manfreda, S., Milella, P. & Portoghese, I., 2009. *Influences of leaf area index estimations on water balance modeling in a mediterranean semi-arid basin*. Nat. Hazards Earth Syst. Sci, 9, 979-991.
- [10] Gutman, G. & Masek, J.G., 2012. *Long-term time series of the earth's land-surface observations from space*. International Journal of Remote Sensing, 33 (15), 4700-4719.
- [11] Hagolle, O., Lobo, A., Maisongrande, P., Cabot, F., Duchemin, B. & De Pereyra, A., 2005. *Quality assessment and improvement of temporally composited products of remotely sensed imagery by combination of vegetation 1 and 2 images*. Remote sensing of environment, 94 (2), 172-186.
- [12] Houborg, R. & Boegh, E., 2008. *Mapping leaf chlorophyll and leaf area index using inverse and forward canopy reflectance modeling and SPOT reflectance data*. Remote Sensing of Environment, 112 (1), 186-202.
- [13] INEA, 1999. "S.I.G.R.I.A. Sistema informativo per la Gestione delle Risorse Idriche in Agricoltura".
- [14] Kaptué Tchuenté, A.T., De Jong, S.M., Roujean, J.-L., Favier, C. & Mering, C., 2011. *Ecosystem mapping at the african continent scale using a hybrid clustering approach based on 1-km resolution multi-annual data from SPOT/VEGETATION*. Remote Sensing of Environment, 115 (2), 452-464.
- [15] Maisongrande, P., Duchemin, B. & Dedieu, G., 2004. *Vegetation/spot: An operational mission for the earth monitoring: presentation of new standard products*. International Journal of Remote Sensing, 25 (1), 9-14.
- [16] Martinez, B., Cassiraga, E., Camacho, F. & Garcia-Haro, J., 2010. *Geostatistics for mapping leaf area index over a cropland landscape: Efficiency sampling assessment*. Remote Sensing, 2 (11), 2584-2606.
- [17] Nemani, R.R., Running, S.W., Pielke, R.A. & Chase, T.N., 1996. *Global vegetation cover changes from coarse resolution satellite data*. Journal of Geophysical Research, 101 (D3), 7157-7162.
- [18] Peng, J., Liu, Z., Liu, Y., Wu, J. & Han, Y., 2012. *Trend analysis of vegetation dynamics in Qinghai–Tibet plateau using hurst exponent*. Ecological Indicators, 14 (1), 28-39.
- [19] Portoghese, I., Iacobellis, V., Sivapalan, M., 2008. *Analysis of soil and vegetation patterns in semi-arid Mediterranean landscapes by way of a conceptual water balance model*, Hydrol. Earth Syst. Sci, 12, 899-911.
- [20] Propastin, P. & Kappas, M., 2012. *Retrieval of coarse-resolution leaf area index over the republic of Kazakhstan using NOAA AVHRR satellite data and ground measurements*. Remote Sensing, 4 (1), 220-246.

- [21] Qiu, B., Zeng, C., Tang, Z. & Chen, C., 2013. *Characterizing spatiotemporal non-stationarity in vegetation dynamics in china using MODIS EVI dataset*. Environmental Monitoring and Assessment, 1-17.
- [22] Sellers, P., 1985. *Canopy reflectance, photosynthesis and transpiration*. International Journal of Remote Sensing, 6 (8), 1335-1372.
- [23] Stenberg, P., Rautiainen, M., Manninen, T., Voipio, P. & Smolander, H., 2004. *Reduced simple ratio better than ndvi for estimating lai in finnish pine and spruce stands*. Silva Fennica, 38 (1), 3-14.
- [24] Telesca, L. & Lasaponara, R., 2005. *Discriminating dynamical patterns in burned and unburned vegetational covers by using SPOT-VGT NDVI data*. Geophysical Research Letters, 32 (21).
- [25] Telesca, L. & Lasaponara, R., 2008. *Investigating fire-induced behavioural trends in vegetation covers*. Communications in Nonlinear Science and Numerical Simulation, 13 (9), 2018-2023.
- [26] Telesca, L., Lasaponara, R. & Lanorte, A., 2008. *Intra-annual dynamical persistent mechanisms in mediterranean ecosystems revealed SPOT-VEGETATION time series*. Ecological Complexity, 5 (2), 151-156.
- [27] Verbesselt, J., Hyndman, R., Newnham, G. & Culvenor, D., 2010. *Detecting trend and seasonal changes in satellite image time series*. Remote Sensing of Environment, 114 (1), 106-115.
- [28] Yin, H., Udelhoven, T., Fensholt, R., Pflugmacher, D. & Hostert, P., 2012. *How normalized difference vegetation index (ndvi) trends from advanced very high resolution radiometer (AVHRR) and système probatoire d'observation de la terre vegetation (SPOT VGT) time series differ in agricultural areas: An inner mongolian case study*. Remote Sensing, 4 (11), 3364-3389.
- [29] Zheng, G. & Moskal, L. M., 2009. *Retrieving leaf area index (lai) using remote sensing: Theories, methods and sensors*. Sensors, 9 (4), 2719-2745.